Hydrogeology Journal
https://doi.org/10.1007/s10040-018-1748-8

PAPER

In situ monitoring of tracer tests: how to distinguish tracer recovery from natural background

V. Bailly-Comte[1] · X. Durepaire[2] · C. Batiot-Guilhe[2] · P.-A. Schnegg[3]

Received: 14 April 2017 / Accepted: 16 February 2018

Abstract
Hydrogeological tracer tests are primarily conducted with fluorescent tracers. Field fluorometers make it possible to monitor tracers at very low concentrations (<1 ppb) and at high frequency. However, changes in natural fluorescence at a site resulting from variations of dissolved and suspended inorganic and organic material may compromise the measurement of useful signals, thereby limiting the chances of identifying or quantifying the real tracer recovery. An elevated natural signal can mask small concentrations of the tracer while its variability can give the impression of a false recovery. This article shows how the use of a combination of several continuous measurements at different wavelengths allows a better extraction of the natural signal. Field multispectral fluorometers were installed at two Mediterranean karst outlets; both drain carbonate systems but have different environmental conditions. The fluorometers functioned over several hydrologic cycles, in periods affected or not by artificial tracers, making it possible to observe natural signal variations at these sites. The optical properties of this type of field fluorometer were used to calculate the spectral response of the different optics of the measuring probe. These responses, superimposed on three-dimensional excitation/emission matrices produced from laboratory fluorescence measurements, allowed an understanding of what the fluorometer sees under natural flow conditions. The result is an innovative method for correcting artificial tracer results. This type of correction makes it possible to fine-tune the effect of natural background variation on tracer recovery curves for a clear identification of the tracer presence and a more precise quantification of its recovery.

Keywords Tracer tests · Multispectral field fluorometer · Karst · Fluorescence · Natural organic matter

Introduction

Tracer testing is a field hydrogeology method commonly used to relate infiltration points to springs or wells, especially in karst terranes (Mull et al. 1988). In addition to its use in geologic and hydrochemical research, this technique is often used to check assumptions related to underground hydraulic connections. Such tracer tests are called qualitative tracer tests and only require a reliable identification of the tracer at the outlet. Besides this, a quantitative analysis of the tracer breakthrough curve (BTC) makes it possible to assess the vulnerability of an outlet with respect to accidental pollution at an infiltration point for the hydrological conditions that exist during the tracer test. Precise analysis of tracer BTCs using mathematical and numerical models can be used to infer porosity and dispersivity properties of the porous media being traced (Kreft and Zuber 1978). Quantitative tracer tests both require a reliable identification and quantification of the tracer.

Fluorescent tracers are widely used due to their very low detection limits (<<1 ppb for uranine) on water samples using a laboratory spectrofluorometer. Field fluorometers can detect the breakthrough of several tracers at springs or wells, with detection limits below 1 ppb for uranine (Schnegg and Dörfliger 1997). The use of an in-situ fluorometer allows measuring the tracer BTC with a short time step, which is its main advantage compared to periodic or manual water sampling. In addition, fluorometer measurements are sometimes the only available data when sample collection is not possible because of too rapid recovery or a site that is not accessible due to flooding. A problem arises however when the background of natural fluorescence gives dubious results, especially during flood events (Lepiller 2001; Meus et al. 2006). This

✉ V. Bailly-Comte
v.bailly-comte@brgm.fr

[1] NRE, BRGM, University of Montpellier, Montpellier, France
[2] HSM, University of Montpellier, CNRS, IRD, Montpellier, France
[3] Albillia Sarl, 2000 Neuchatel, Switzerland

Published online: 20 March 2018

natural fluorescence may also limit the quantification of the tracer concentration, especially for low concentrations arriving late during the tracer BTC. Accurate results are needed to describe the tailing effect at the end of the tracer BTC because it is used to determine the hydrodispersive properties of the ground media (Becker and Shapiro 2003).

As a result, a methodology is needed to address the two main issues when dealing with in-situ fluorometers:

- Detection: Is the tracer really present in the water?
- Quantification: To which extent does the natural fluorescence influence the measurements?

In-situ multispectral fluorometers dedicated to dye tracing techniques or biological monitoring can measure fluorescence in water at several wavelengths. Most fluorometers (Turner designs, Sea-Bird Scientific, GGUN fluorometers from Albillia) use an optics system made of a combination of light-emitting diodes (LEDs), photo-detectors and filters to limit the range of emitted and excitation wavelengths. As a result, each signal measured by a multispectral fluorometer describes the diffusion and fluorescent properties of the water in the optical cell for a given range of excitation and emission wavelengths. When conducting a tracer test, the signal measured by a multispectral fluorometer may have four origins:

- The light emitted by the fluorescence of the tracer, which constitutes the true signal and indicates the passage of the tracer.
- A fraction of excitation light scattered by the water and suspended matter (SM), which depends on the size and color of this material (Sadar 2004). The type of SM depends on the study site. It varies depending on hydrological conditions (Lacroix et al. 2000).
- The light emitted by fluorescence of substances other than the tracer that are present in the water being analyzed. Among naturally fluorescent substances present in groundwater, natural organic material (NOM) contains numerous fluorophores. Among these fluorophores, two humic-like compounds called peak A and peak C type are naturally originated from the leachate from soil (Smart et al. 1976; Coble 1996; Baker et al. 1997; Hudson et al. 2007; Batiot-Guilhe et al. 2008; Lapworth et al. 2009; Blondel et al. 2010; Mudarra et al. 2011). Also found are protein-like compounds derived from fresh organic matter or microbial production that may come from organic effluents (Lapworth et al. 2008; Batiot-Guilhe et al. 2008; Blondel 2008; Mudarra et al. 2011; Quiers et al. 2013). To date, fluorophores as a group have fluorescent properties ranging from the mid ultra-violet (UV) to indigo light (from 220 to 450 nm). They have fluorescent characteristics similar to short wavelength tracers and interfere particularly with the recovery signal of artificial tracers such as sodium naphthionate, amino-G-acid (AGA), tinopal and uranine.
- Finally, water and SM absorb a fraction of diffusion and fluorescent lights. This absorbance is strong in the UV and tends to decrease as a function of the wavelength. Its intensity depends on the size and the color of the SM (Sadar 2004).

The last three components constitute what is called natural background when measuring a tracer recovery. Although fluorescent tracers can be considered non-toxic, hydrogeologists are encouraged to minimize as much as possible the quantities they inject. This reduces the concentrations measured at the recovery point, increasing the relative importance of natural background. An elevated natural signal can mask small concentrations of the tracer while variability of the natural signal can give the impression of a false recovery. In addition, in case of a multitracer test, artificial fluorescence from another tracer may affect the measured signal. This last noise referred to an artificial background noise that can also lead to erroneous conclusion.

This study focuses on the distinction between the real signal and the combined effect of the three naturally occurring signals (NOM fluorescence, SM diffuse reflections and absorption) that can affect in-situ measurements by multispectral fluorometer. A new method to distinguish tracer recovery from natural background is described, with an application to a long-term monitoring of natural fluorescence background and two tracer tests addressing qualitative and quantitative issues.

Materials and methods

Previous approaches for natural background correction

Schnegg and Flynn (2002) describe in detail a turbidity correction to account for natural background due to scattering of suspended materials during tracer recovery. The method requires at least the use of a multispectral fluorometer that measure turbidity and tracer recovery with two independent optics systems. Water samples of increasing turbidity (1, 10 and 100 NTU) are used to calibrate the turbidity optics system, and to measure the influence of turbidity on the optics system that measures the tracer recovery. The relationship between turbidity and measured signals is used at each time step to compute the amount of stray signal due to naturally occurring turbidity. Finally, this stray signal is subtracted from the measured tracer signal to get the corrected signal of tracer recovery. The turbidity signal measured with standard solution may however be different from the ones produced by suspended materials in natural water, which is why this correction can be weighted by

a parameter called "turbidity sensitivity" (TS), as proposed by the FLUO software (Albillia) when analyzing fluorescence measurements from GGUN fluorometers.

Schnegg and Le Doucen (2006) propose to use the optics system designed for the monitoring of optical brighteners as a proxy of the natural fluorescence of NOM. Their method, called DOM (dissolved organic carbon) correction, allows for correction of a signal of uranine recovery from an increase of stray signals due to NOM fluorescence. The signal measured by the optics system measuring optical brighteners is expressed in ppb equivalent of tinopal tracer. This requires, first, removal of the effect of the uranine recovery on the tinopal equivalent signal, which is done by a mathematical inversion proposed by Schnegg and Thueler (2012). Then, the resulting tinopal time series is supposed to be a linear function of the stray signal due to NOM measured by the uranine optics system. This stray signal is subtracted from the measured tracer signal to get the corrected signal of uranine recovery. The linear coefficient between tinopal and uranine stray signals is manually adjusted to reduce the correlation between the tinopal (in ppb equivalents) and uranine (in ppb) time series. It can be noticed that the same results will be obtained if the NOM fluorescence is expressed in the ppb equivalent of AGA since the raw measurements are done with the same optics system.

These previous methods can thus be used to reduce the effect of turbidity on tracer recovery, or reduce the effect of NOM fluorescence when using uranine as a tracer. They can be combined for an uranine tracer test, but this requires arbitrarily adjustment of one parameter each. To the author's knowledge, there is no method that can correct the effect of NOM fluorescence when using a different tracer than uranine. In addition, these corrections can be doubtful in case of highly disturbed signals due to high variation of natural background, because they require the manual adjustment of a parameter.

Multioptics correction method: background correction based on a multispectral monitoring

This new method has been developed for a four-optics-system multispectral fluorometer that can simultaneously record

- The fluorescence of water on three ranges of excitation and emission wavelengths
- The fluorescence at 650 nm along the Rayleigh diffusion spectrum to measure the turbidity of water independently from artificial tracer recovery (Schnegg and Flynn 2002)

The first step is to identify the range of excitation/emission wavelengths that are measured by the multispectral fluorometer. The optical characteristics of the excitation LEDs, filters, and photodiodes of the fluorometer are used to compute the spectral response of the signals measured by each optics system. These spectral responses are normalized so that the maximal intensity of excited or emitted light is one. This procedure can be realized for each optics system of the multispectral fluorometer to describe the spreading of the spectral bandwidth, knowing the spectral characteristics of each combination of LEDs and photodiodes and their associated filters. The procedure is applied in Fig. 1 in the case of the rhodamine optics system (510 nm) from a GGUN fluorometer, leading to isolines that represent the percentage of fluorescence intensity recorded by the fluorometer for a given emission (X-axis) and excitation (Y-axis) wavelength. This step allows checking the absence of overlap between spectral responses of the different optics system that are used by the fluorometer. It is also used in the following to compare the spectral characteristics of each optics system with those of turbidity and NOM fluorescence based on water samples analyses with a laboratory spectrofluorometer.

Under natural conditions, the measurement between the different optics systems is correlated to two parameters: fluorophores present in the NOM, and SM simultaneously playing a diffusive role and an absorption role on the light. This correlation results from the wide measurement windows of the optics system of the fluorometer (Fig. 1). The new correction method described in this section consists of quantifying the signal of one optics system using a linear combination of all the other optics system. With (U_j) as the measurement of an optics system, it is possible to define a model of this measurement ($\hat{U}_j$) by linear combinations of measurements recorded simultaneously by other optics system (U_i), including the turbidity optics system ($i = 1$ to 4, $i \neq j$, Eq. 1):

$$\hat{U}_j(t) = \sum_{i=1, i\neq j}^{4} \beta_i \times U_i(t) + \gamma \quad (1)$$

The measurements U_i are the fluorometer time series expressed in turbidity units (NTU) for the turbidity optics system (650 nm), and in equivalent concentrations of tracer for the other optics system. Then, the simulated signal $\hat{U}_j$ is subtracted from the measured signal U_j to assess the corrected recovery.

The two parameters β and γ are automatically adjusted to minimize the sum of the squared residuals between the real measurement (U_j) and its estimate ($\hat{U}_j$) over a calibration-measuring period, called the initialization period in the following. This initialization period has to be chosen outside of a period influenced by an artificial tracer, so as to have the most reliable estimation of the real measurement.

The main steps of the multioptics correction method are summarized in Fig. 2. The fluorometer measures four distinct signals, one (U_1, Fig. 2) being measured by the optics system $O1$ dedicated to the tracer to quantify. The signal U_1 is directly converted to ppb as recommended by the fluorometer technical guide, while the signals U_2 and U_3 are

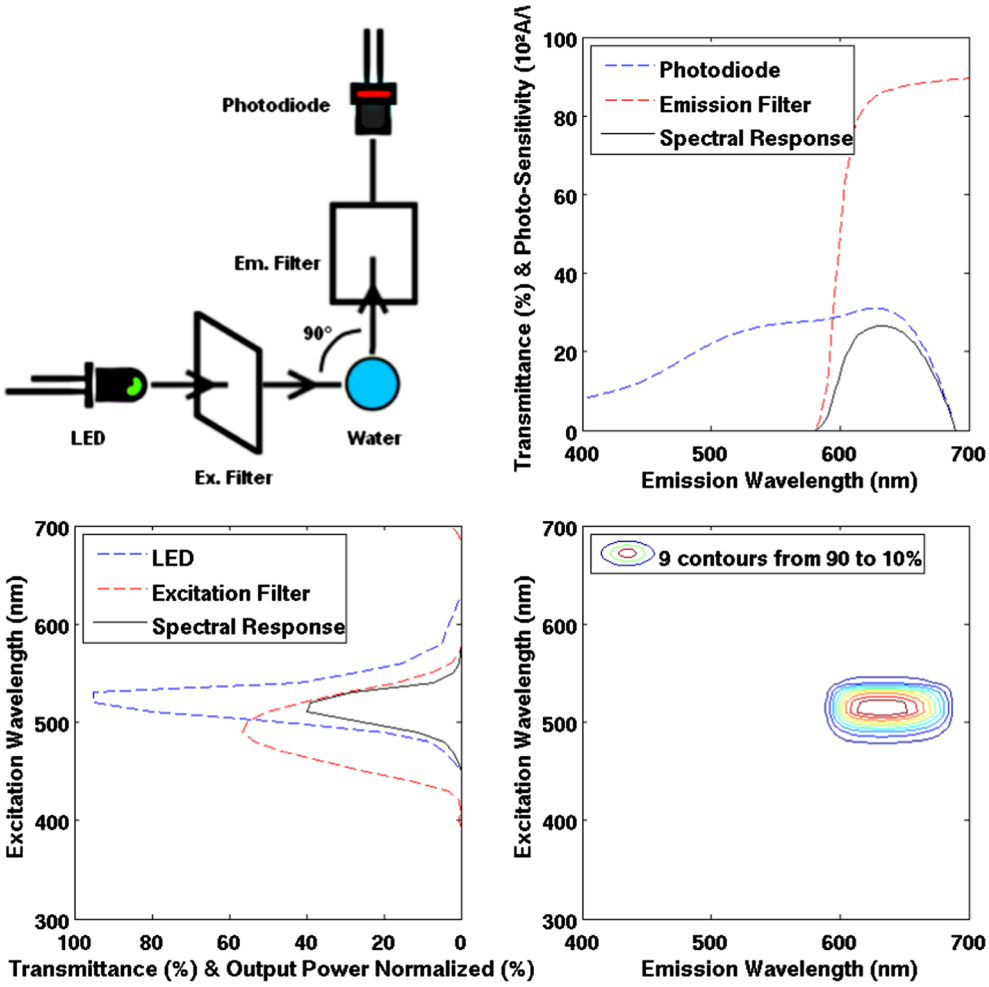

Fig. 1 Normalized spectral response of the GGUN fluorometer reported in an EEM. The figure shows the spectral characteristics of the LED, the filters and the photodiode with the example of the rhodamine optics system

converted to ppb after having removing the effect of the tracer recovery following the tracer separation method given by Schnegg and Thueler 2012. This effect may however be low enough to be neglected. Then, the multioptics correction method consists of fitting the parameters β and γ in Eq. (1) over an initialization period. These parameters are used to compute the natural background during the tracer recovery, which is subtracted from the measured signal U_1 to get the corrected recovery.

Application to the Lez and Fontaine de Nîmes (FdN) catchments

Long-term fluorescence monitoring

The study is based on a comparison of periodic long-term fluorescence monitoring using a laboratory spectrofluorometer at the Lez Spring (identification number BSS002GNMG; BRGM 2017a), and several time series recorded by GGUN in-

		Three optics used for tracer recovery				Turbidity
1. In-situ measurements	Optics	O1	O2	O3		O4
	Raw data (mV)	mV_1	mV_2	mV_3		mV_4
2. Calibration	Raw tracer signals (ppb)	U_1	U_2	U_3	Turbidity signal (NTU)	U_4
3. Multi-optics correction	Background simulation	Selection of the initialization period	$\hat{U}_1 = f(U_2, U_3, U_4)$ (Eq. 2)			
	Corrected tracer signal	U_1-$\hat{U}_1$				

Fig. 2 Schematic workflow and data post processing from raw data of a multispectral field fluorometer (four optics system) to corrected recovery according to the multioptics correction; example of tracer recovery measured by the first optics system O1

situ fluorometers that continuously measure fluorescence at the Lez and Fontaine de Nîmes (FdN) springs (identification number BSS002ESPJ; BRGM 2017b). These two sites are part of the French Karst observatory network. The Lez Spring is also part of the MEDYCYSS observatory (Jourde et al. 2011).

The FdN Spring is the primary outlet of the FdN karst system (Maréchal et al. 2008), which is composed of urgonian Cretaceous limestone. Its recharge area is partially urbanized in its downstream part, leading to evidence of anthropogenic impacts on the groundwater resource (Maréchal et al. 2004). The discharge of the FdN Spring is relatively limited in low-flow conditions (<50 L/s) but can exceed 15 m^3/s during flash floods. A GGUN-FL24 (No. 645) fluorometer with four optics system has been installed at the FdN Spring since 2012. These optics system are designed to measure uranine or eosin at 470 nm, any rhodamine (sulfo-, amido-, -WT) at 525 nm, optical brighteners like AGA or tinopal at 365 nm and turbidity at 650 nm along the Rayleigh spectra. These optics systems are denoted as being either uranine, rhodamine, AGA and turbidity in the following.

The Lez Spring is the main outlet of the Lez karst system, which is composed of Jurassic limestones and Cretaceous (Berriasian) marly-limestone, located north of Montpellier, France (Thiery and Berard 1984, Maréchal et al. 2014). Groundwater is abstracted directly from the main karst conduit upstream from the spring. This induces a lowering of the water table and groundwater depletion that is recharged in autumn. As a result, part of the pumping water is redirected to the natural stream in order to maintain hydrological and biological functioning of the surface stream. This active groundwater management scheme also has a positive impact on flash-flood mitigation, the karst aquifer acting has a flood storage tank (Fleury et al. 2009; Jourde et al. 2014). The discharge of the Lez Spring is fixed to a minimal rate of 160 L/s in low flow conditions and can reach 16 m^3/s in high flow conditions (Marechal et al. 2014). This spring supplies water for Montpellier and its surroundings. The recharge area of this karst system is predominantly rural and well protected, with low anthropogenic pressure (Leonardi et al. 2013). A GGUN-FL24 fluorometer (No. 298) was installed at the Lez Spring in 2010, and was upgraded in 2014 to a customized GGUN-FL30 (No. 918) fluorometer in which a low-wavelength optics system (285 nm) replaced the common rhodamine optics system. This optics system was installed to monitor natural NOM fluorescence of the proteic-like type; it is called the 'proteic optics system' in this article. The other optics systems are the same as those used at the FdN site.

Tracer tests dataset

Two tracer tests were studied to compare the different SM and NOM correction methods, one at the Lez Spring and the other at the FdN Spring. On 13 November 2014, 1.5 kg of uranine was injected into a sinkhole in a temporary watercourse, the Terrieu, about 5 km northeast of the Lez Spring. A rain event from 15–16 November 2014, with a rainfall total of about 30 mm on the recharge area, produced a water level rise and rapid circulation of water within the system, with a large influx of SM and NOM accompanying the tracer recovery. The spring reached a discharge of 4.6 m^3/s during the tracer recovery. The main focus of this tracer test was to determine how the tracer recovery can be precisely computed from the different signals measured by the fluorometer (quantitative tracer test analysis).

On 4 December 2013, 100 g of sulforhodamine B were injected into the Puits des 9 arcades (identification No. BSS002ESQL; BRGM 2017c) located in the recharge area of the FdN Spring The tracer, originally trapped within a cavity disconnected from the system, was mobilized after a major rain event from 18–19 January 2014. This event produced a cumulative rainfall of about 70 mm on its recharge zone, which in turn induced a water level rise and rapid circulation of water within the karst system, with a large influx of SM and NOM. The main question relative to this tracer test is whether the tracer is actually present (qualitative tracer test analysis).

Results

Comparison of multispectral fluorometer spectral windows and natural background spectral characteristics measured by a laboratory spectrofluorometer

Figure 3a shows the spectral responses of the GGUN fluorometers used at these two sites. These spectral windows are reported on a theoretical excitation-emission matrix (EEM), which shows the fluorescence intensity emitted by the water sample at given excitation and emission wavelengths (Coble 1996). The Rayleigh diffusion spectrum corresponds to the "turbidity area" along a 1/1 slope on the EEM, i.e. diffusion where emission wavelength equals excitation wavelength. The theoretical first order Raman spectrum is also shown between two black dashed lines, as well as the second order Raman spectrum. The green-shaded area corresponds to the domain of NOM fluorescence (Coble 1996; Hudson et al. 2007). This is the specific spectral response of the water molecule due to Raman diffusion (Zepp et al. 2004). It can be concluded that the AGA spectral window falls in the NOM fluorescence area, the fluorometer's turbidity spectral window overlaps the turbidity area (between 600 and 700 nm) and that the uranine and rhodamine spectral windows are theoretically not affected by Rayleigh diffusion or NOM fluorescence; they do however overlap the domain of the first order Raman spectra.

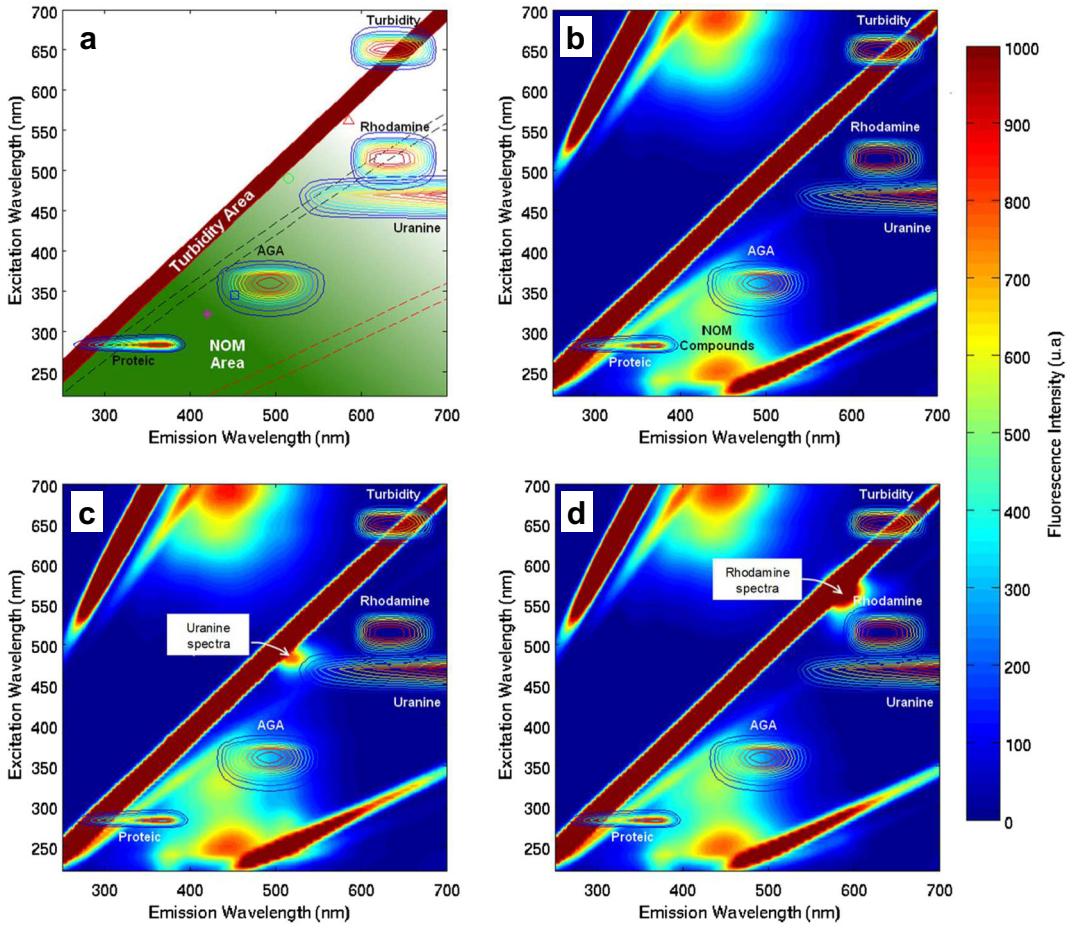

Fig. 3 Normalized spectral responses of the five optics system of the GGUN multispectral fluorometer used in this study plotted on: **a** a theoretical EEM showing Rayleigh, Raman spectra and a green shaded area corresponding to the domain of Natural Organic Matter fluorescence; **b** an EEM obtained at the Lez Spring on 21 September 2015; **c** the same EEM as **b** with addition of uranine; **d** the same EEM as **b** with addition of sulforhodamine B

These spectral windows are also reported on a real example of EEM obtained at the Lez Spring on 21 September 2015 (Fig. 3b), i.e. without tracer addition. The fluorescence spectra were recorded using a SHIMADZU RF-5301 PC (xenon lamp) 3D spectrometer. The temperature was stabilized at 20 °C in a bath with a thermostat because fluorescence is temperature-dependent. NOM fluorescence was measured in a 1-cm quartz fluorescence cell. Each EEM was generated by scanning excitation wavelengths from 220 to 450 nm at 10 nm steps and detecting the emitted fluorescence between 250 and 550 nm at 1 nm steps. Slit-widths of 15 nm were used for the monochromators with a fast default scan speed (Batiot-Guilhe et al. 2008; Quiers et al. 2013).

Figure 3b shows that the NOM compounds influence both the AGA and proteic optics system. This EEM shows that the AGA optics system can measure the humic-like peak fluorescence of the organic matter, while the proteic optics system is closer to the proteic-like peak of the organic matter. This distinction is important at the Lez karst system, since it has been shown that the proteic-like peak is related to fast infiltration waters that carry pulses of bacterial contamination (Quiers et al. 2013; Durepaire et al. 2014; Erostate et al. 2016). Figure 3b also shows that the fluorescence domain of the NOM compounds spreads over a wide range of emission wavelengths, so that the high intensity of NOM compounds also falls within the Raman spectral domain. The Raman spectrum can be followed for higher wavelengths until approximately the uranine spectral window, which explains how NOM fluorescence can affect the uranine signal measured by the fluorometer.

Finally, Fig. 3c,d shows EEMs measured on the same water, but with an arbitrary addition of uranine or sulforhodamine B. These figures show graphically how the spectral windows intercept the spectral response of these two tracers and highlight that the spectral window of the GGUN fluorometer overlaps only a small part of the tracer signal.

To conclude, the spectral window of the AGA and proteic optics system overlap the NOM fluorescence domain, while the uranine and rhodamine spectral windows fall between the turbidity and the NOM fluorescence domains. The EEM

representation given by Fig. 3b shows that the three optics system designed for tracer measurements of the GGUN fluorometer can be influenced by the two origins of natural background, i.e. turbidity (for all optics system) and NOM fluorescence (mainly the AGA and proteic optics system).

Natural fluorescence monitoring using a multispectral fluorometer

Figure 4c–e shows the raw in-situ fluorometer (GGUN-FL24 No. 645) time series fluorescence recorded at the FdN Spring during two large flood events in September and October 2014. These measurements are compared to the discharge time series (Fig. 4b), which exceeded 15 m^3/s during the second flood event. These large flood events occur in autumn after a relatively long dry season. Daily rainfall data are recorded at the Nîmes-Courbessac Météo France station (Fig. 4a, identification No. 30189001).

Turbidity measurements show very high variation, exceeding 100 NTU for the second event (Fig. 4b). The AGA optics system time series also shows a very high response that reached 400 ppb equivalent of AGA during the first flood event, while a very small fluctuation was measured during the second event. This means that the second flood, which is a larger flood event, brings a lot of turbidity with few fluorescent NOMs, while the first flood event may have primarily carried

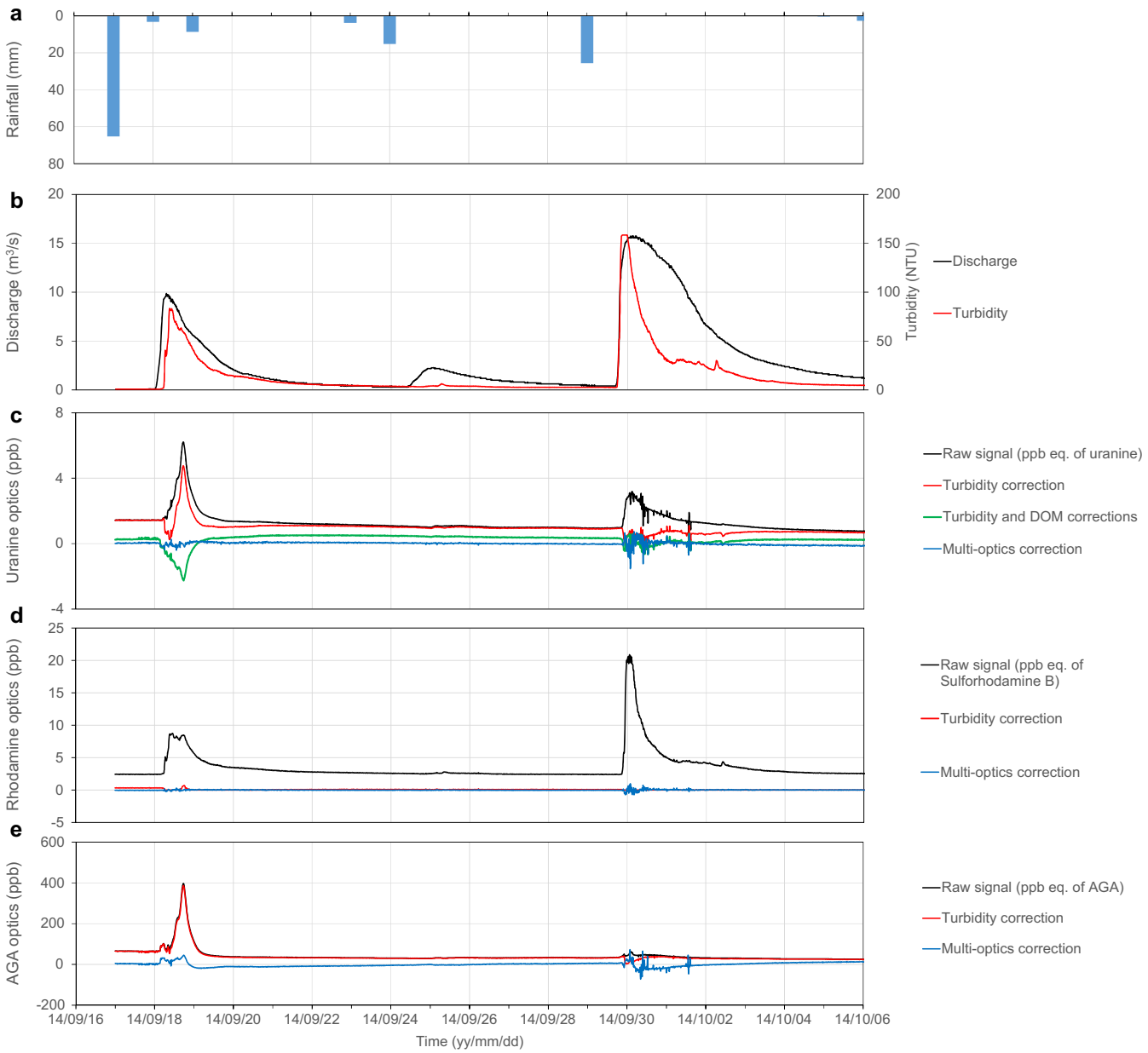

Fig. 4 Discharge time series compared for raw and corrected fluorescence time series from an in-situ fluorometer (GGUN-FL24 No. 645) at the FdN Spring: **a** rainfall, **b** discharge, **c** uranine optics system, **d** rhodamine, **e** AGA optics system

anthropogenic organic matter stored in the vadose zone during the summer, which is consistent with the land cover of this urbanized karst system.

In addition, turbidity dynamics are also clearly observed on the rhodamine optics system, at a value close to 20 ppb equivalent of sulforhodamine B, while a combination of the AGA and turbidity time-series is observed on the uranine optics system, which reaches 6 ppb equivalent of uranine during the first flood event. As expected, uranine and rhodamine optics system measure a natural background that results from both turbidity and NOM fluorescence.

The turbidity sensitivity (TS = 1) parameter was used to correct the effect of turbidity in Fig. 4c–e (see the turbidity correction time series in red). This correction gives very good results for the rhodamine optics system since the corrected signal is close to zero, as expected without tracer. Thus, for this optics system, the natural fluorescence background is controlled primarily by turbidity diffusion, which is consistent with the position of the rhodamine spectral window in Fig. 3b. The spectral window of the rhodamine optics system is far from the NOM fluorescence domain and close to the turbidity area, which explains why the natural fluorescence background has less influence than the turbidity background in this optics system. This correction however does not remove the natural fluorescence background signal that is measured on the uranine and AGA optics system.

The DOM correction proposed by Schnegg and Le Doucen (2006) has been applied to the uranine optics system on corrected signals from turbidity (TS = 1). The results are shown as a green line in Fig. 4c. This correction gives better results than the use of the turbidity sensitivity alone since the corrected signal is lower, but a large underestimation (negative signal) appears during the first flood event where NOM fluorescence is high. This means that the natural fluorescence background measured by the uranine optics system is controlled by turbidity diffusion and natural NOM fluorescence, which is consistent with the position of the uranine spectral window in Fig. 3b.

The results of the multioptics correction are shown as blue lines in Fig. 4c–e. This correction allows removal to the greatest extent the background noise on each of the optics system. It is furthermore the only method that proposes a NOM and turbidity correction of an optics system using a combination of the measurements from the three others optics system. The quality of the model comes from the fact that no peak is forgotten or generated. Within the framework of artificial tracing, a considerable reduction in natural perturbation is thus possible without amplification or addition of artifact peaks. A comparison of the results given by DOM correction and the multioptics correction is shown in Fig. 5 for the uranine optics system (there is no DOM correction for the others optics system), which clearly highlights that the natural background is better simulated with the multioptics correction.

Tracer test applications

Application to the Lez Spring

Figure 6 shows uranine recovery monitoring at the Lez Spring using a multispectral fluorometer (GGUN-FL30 No. 918). Black (Fig. 6c) and red (Fig. 6b,c) time series show raw data converted to ppb of uranine with (TS = 0.7) or without (TS = 0) turbidity correction respectively. The value of TS = 0.7 provides the best correction of turbidity based on a visual inspection of the uranine recovery versus the turbidity time series. This value has been fixed for all other computations. Two simulated natural backgrounds are compared in Fig. 6b using the DOM and turbidity corrections in green (Fig. 6b, TS = 0.7), and the multioptics correction in blue. The parameters used for these corrections (Eq. 1) are fitted

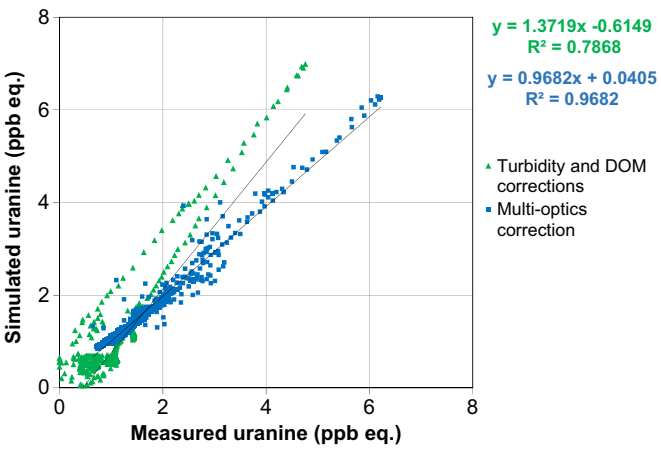

Fig. 5 Correlations between simulated and measured signals from the uranine optics system for the DOM (after turbidity correction) and multioptics correction methods for the times series shown in Fig. 4c

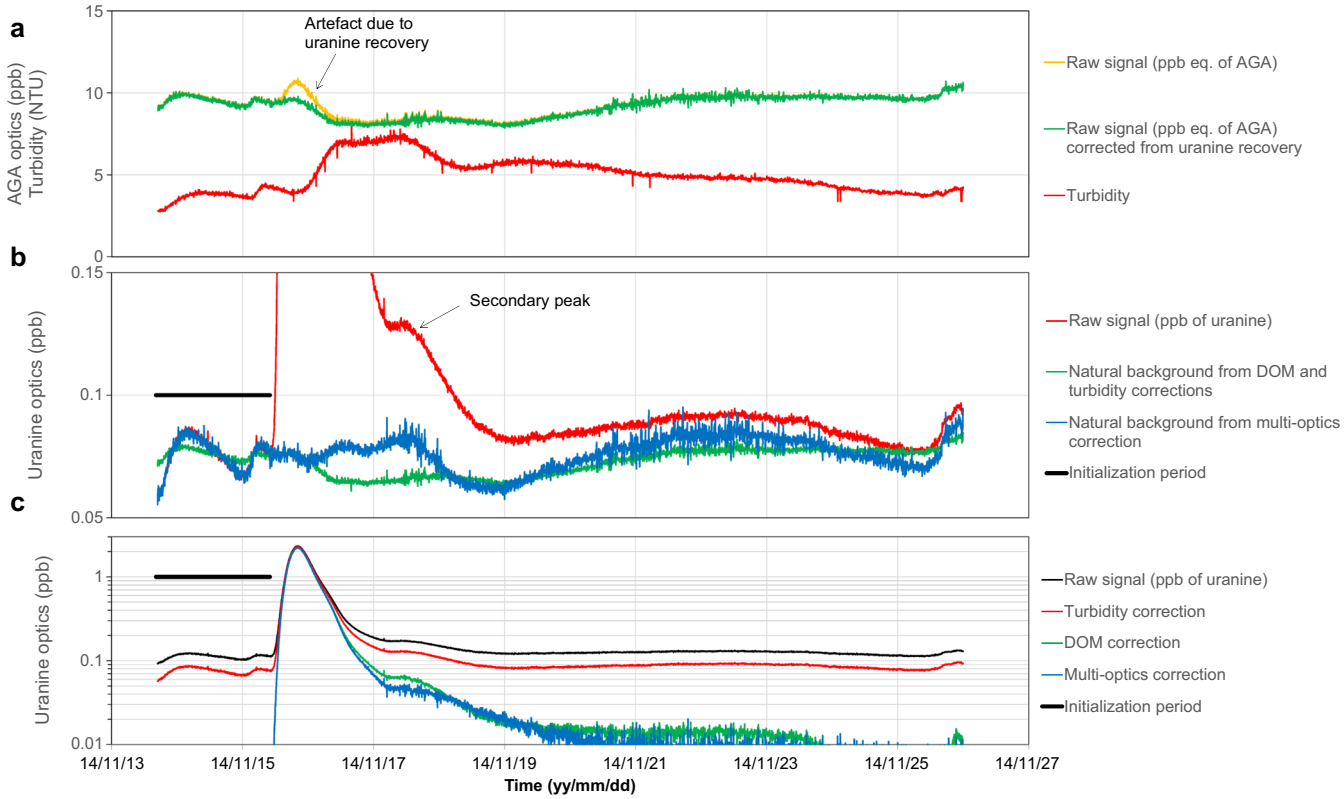

Fig. 6 Recovery curves from the uranine tracer test at the Lez Spring (November 2014) with: **a** calibrated data for the AGA and turbidity optics system; **b** simulation of natural background noise by the DOM and multioptics corrections methods; **c** raw and corrected recovery curves (semi-log)

during the initialization period shown in Fig. 6b,c (2 days) with a thick black line.

An artifact peak appears during the maximum uranine recovery on the signal measured by the AGA optics system (Fig. 6a). This means that the influence on the uranine recovery has to be removed following the tracer separation method (Schnegg and Thueler 2012), which gives the green time series (Fig. 6a).

The DOM correction does not converge towards the non-corrected measurement at the end of recovery (Fig. 6a) but generates a slight overestimation of the tracer recovery. Figure 6b also shows that the natural background is well simulated during the initialization period for the multioptics correction, while some differences between simulated and measured signals can be seen using the DOM correction. Indeed, Fig. 7 shows that the relationships between the simulated and the measured signals during the initialization period follows a linear relationship with a slope close to 1 (0.92) and a high correlation coefficient (R^2 = 0.92) for the multioptics correction, while the DOM correction cannot be used to reproduce all the dynamics of the natural background (slope of 0.24 with R^2 = 0.72).

Finally, the secondary peak shown in Fig. 6b on the raw uranine signal seems to be mainly related to an increase of the natural background noise, as shown by the evolution of the natural background computed by the multioptics correction method. This conclusion cannot be given with the use of the DOM correction method. As a result, the multioptics correction method provides a finer estimate of background noise, which can be subtracted from the raw tracer signal to get the corrected tracer recovery.

Application to the FdN Spring

Figure 8c shows monitoring of sulforhodamine B recovery at FdN Spring using a multispectral fluorometer (GGUN-FL24 No. 645), along with rainfall (Fig. 8a), discharge data at the spring and water depth in the sinkhole where the tracer was injected (Fig. 8b). The water-depth time series show that the tracer injected on 4 December 2013 was carried by karst groundwater after the rain event of 18–19 January 2014. Following precipitation on 18–19 January 2014, in response to the flood, the measurements in ppb from the rhodamine optics system of the GGUN (in black, Fig. 8c) show three distinct peaks. Two corrections were made on this tracer test in order to isolate the tracer signal from the natural background:

– The turbidity correction in red using the FLUO software (Schnegg and Flynn 2002). This correction is obtained

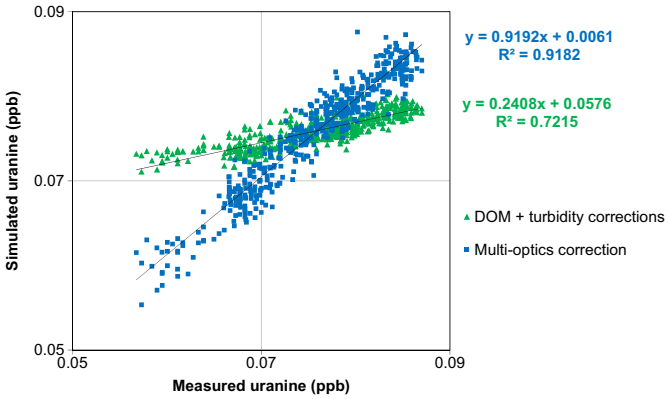

Fig. 7 Correlations between the simulated and measured signal from the uranine optics system for the AGA and multioptics method for the initialization period shown in Fig.6

through the optimization of the turbidity sensitivity coefficient (TS), evaluated here at 0.7 for an optimal correction. The turbidity correction allows for removal of most of the stray signal, especially for the third peak, but the first and second peaks are still there with a similar intensity.

– The multioptics correction method in blue, which uses data from the uranine, turbidity and AGA optics system expressed in ppb equivalent of tracers. A correction for the influence of the tracer recovery on the other optics system was not needed here due to the very low recovery. Simulation of natural background noise shows that the first and third peaks are removed by the multioptics correction. These peaks result from variations of natural background (Fig. 8c, see the purple time series). The second peak is not explained by the evolution of the natural background, which means that this peak represents a fast restitution of the tracer due to the flood event.

No DOM correction can be made here since this method was only dedicated to the uranine optics system. If the aim of this correction was to validate the presence of the tracer, some basic computations can be made to see if the resulting tracer

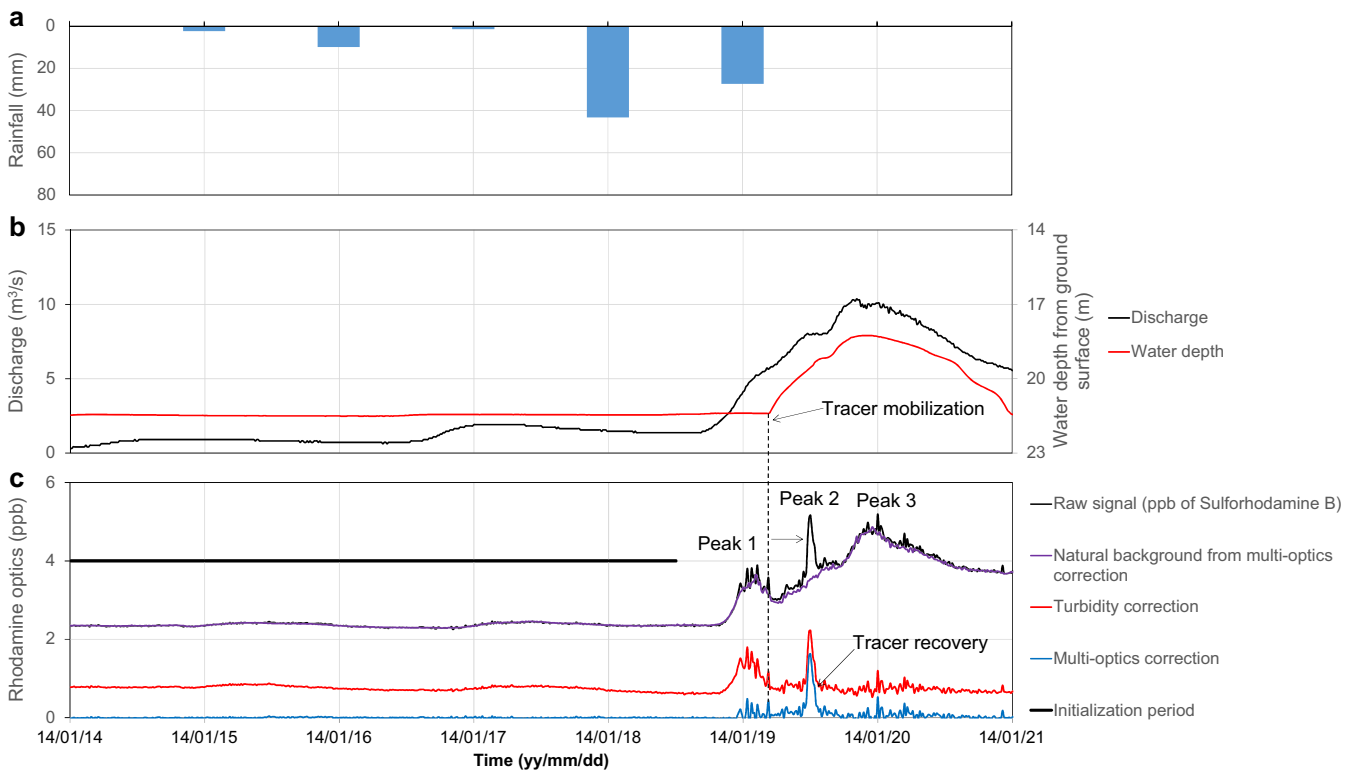

Fig. 8 Tracer recovery curve of sulforhodamine B at FdN with: **a** daily rainfall; **b** discharge at the FdN Spring and water depth evolution in the injection point; **c** natural background simulated by the multioptics correction, and recovery curves corrected by the turbidity and the multioptics corrections. The dashed line represents the time when the tracer was moved from the injection point due to the flood event

recovery gives coherent quantitative information. The total recovery is extremely short (3 h) and occurred between 11 and 14 h on 19 January 2014. The estimated tracer recovery rate is between 60 and 70%, and the average flow velocity in response to the flood was estimated at 110 m/h. Without this treatment, it would have been impossible to identify tracer recovery because of the high variability of natural fluorescence and turbidity during this flood event. This result shows that the multioptics correction method makes it possible to separate the natural signal from tracer recovery, avoiding incorrect interpretations, even when the natural background is of the same order of magnitude as the tracer signal.

Discussion

Natural background noise correction using the multioptics method neither forgets nor generates any artifact peak; its use considerably improves the evaluation of the recovery curve when using a multispectral fluorometer. The assessment of background noise allows for measurement of a late tailing effect on tracer recovery with greater precision, which may have an influence on main tracer BTC characteristics (mean residence time, recovery rate) when NOM fluorescence and turbidity increase relative to the tracer concentration. For instance, this new method allows for an understanding of the origin of a second tracer recovery peak (see Fig. 6), which is mainly due to variation in natural fluorescence or light diffusion due to suspended materials.

The use of this new method does not require an arbitrary evaluation of parameters and can be done automatically as soon as the user identifies the initialization period. As a result, the quality of the natural signal estimate only depends on the choice of the adjustment period. It is thus recommended to use the in-situ multispectral fluorometer prior to and/or, if nothing else, after several days of tracer recovery. The ideal is to have significant variations in background noise parameters during the adjustment period, thus preferentially during flood events. The adjustment period can be split up; for example, it may be judicious to do the adjustment on several floods while leaving out the record of less representative intermediate data. This choice must rest on knowledge of correlations and overlap between the different optics system of the multispectral fluorometer (Fig. 2) and on an understanding of the parameters of natural background noise at the site under study. This approach can be used with any types of in-situ multispectral fluorometer as long as the latter simultaneously measures the fluorescence at various wavelengths and turbidity.

Results obtained in the course of this study relate to periods in which flash-flood events occurred. These are episodes of high-intensity precipitation over a short time period (Braud et al. 2014). On karst, this type of episode causes rapid circulation and elevated discharges (Bonacci et al. 2006; Bailly-Comte et al. 2009), and generates infiltration fluxes that mobilize SM and NOM from the soils and the vadose zone. This type of karst flash flooding is common in the Mediterranean region. During artificial tracer tests, this leads to high variation in the fluorescence signals ascribed to natural background, and to short recoveries that require high-frequency monitoring. This problem is even more common regarding karsts with polyphase structures (Fleury et al. 2013), in the case where the tracer is trapped within a cavity disconnected from the karst system, which is the scenario found during tracing at the FdN site. Starting again with a large flood, rapid circulation of the water mobilizes the tracer and drains SM and NOM to the outlets. The result is rapid recovery with major perturbation of the fluorescence signal. This example shows that this new correction allows rigorous study using tracer tests even under extreme recovery conditions, i.e. when it is not possible to collect samples at a suitable sampling rate.

Conclusion

In-situ fluorometer monitoring of artificial tracers is becoming more widely used. These devices monitor different tracers continuously at very low concentrations, in places where manual sampling may be impossible because of too rapid tracer recovery or difficult access in flood conditions. In looking for a tracer on measurements recorded by the in-situ fluorometer, the raw signal recorded is the sum of two components: the effective recovery of the tracer of interest, and the natural signal due to variations of SM and fluorescent NOM. When identification by sampling and analyzing the fluorescence in a laboratory is not possible, the signal registered by the field fluorometer can be misleading: an elevated natural signal can mask low concentrations of the tracer, whereas a variable natural signal can give the impression of a recovery which is false. By combining the measurements of several optics system, the multioptics correction method makes it possible to evaluate the natural signal independently of the tracer of interest. A considerable reduction in natural perturbation is thus possible without amplification or addition of artifact peaks, which leads to a better identification or quantification of the tracer in water. Long-distance tracer tests with reduced tracer injection masses or low recovery rates can be measured with precision even in zones of high natural fluorescence and high turbidity. This procedure greatly improves results obtained from artificial tracing during flood events accompanied by highly variable NOM and SM.

Acknowledgements This work was performed within the framework of the Lez and Fontaine de Nîmes observation sites, both part of the KARST observatory network (www.sokarst.org) initiative from the INSU/CNRS (French National Institute for Earth Sciences and Astronomy), which aims to strengthen knowledge-sharing and promote cross-disciplinary research on karst systems. We also thank Pascal Brunet and Véronique

Leonardi for their help with in-situ fluorometer measurements at the Lez Spring.

Funding Information This work benefitted from financial support from the MEDYCYSS observatory (OSU OREME, Mediterranean Environment Research Observatory, https://oreme.org/services/observation/karst/medycyss), the SNO KARST network and an internal project of the BRGM (project No. RP16D3E014).

References

Baker A, Barnes WL, Smart PL (1997) Variations in the discharge and organic matter content of stalagmite drip waters in Lower Cave, Bristol. Hydrol Process 11:1541–1555

Batiot-Guilhe C, Seidel JL, Cordier MA, Van-Exter S, Bicalho C, Lafare A, Rodier C, Jourde H (2008) Characterisation of underground flows in karstic aquifers by studying DOM fluorescence example of two Mediterranean systems (Lez and Causse d'Aumelas, south-eastern France), 13th IWRA World Water Congress, 1–4 September, Montpellier, France

Becker MW, Shapiro AM (2003) Interpreting tracer breakthrough tailing from different forced-gradient tracer experiment configurations in fractured bedrock. Water Resour Res 39(1):1024. https://doi.org/10.1029/2001WR001190

Bailly-Comte V, Jourde H, Pistre S (2009) Conceptualization and classification of groundwater–surface water hydrodynamic interactions in karst watersheds: case of the karst watershed of the Coulazou River (southern France). J Hydrol 376:456–462

Blondel T (2008) Traçage spatial et temporel des eaux souterraines dans les hydrosystèmes karstiques par les matières organiques dissoutes Expérimentation et application sur les sites du Laboratoire Souterrain à Bas Bruit (LSBB) de Rustrel – Pays d'Apt et de Fontaine de Vaucluse [Spatial and temporal tracing of groundwater in karstic hydrosystems by dissolved organic matter: experimentation and application on the sites of the Low Noise Underground Laboratory (LSBB) of Rustrel - Pays d'Apt and Fontaine de Vaucluse]. PhD Thesis, Université d'Avignon et des Pays du Vaucluse, Avignon, France, 186 pp

Blondel T, Emblanch C, Dudal Y, Batiot-Guilhe C, Travi Y, Gaffet S (2010) Transit time environmental tracing from dissolved organic matter fluorescence properties in karstic aquifers: application to different flows of 'Fontaine de Vaucluse' experimental basin advances in research. Karst Media 1:143–149

Bonacci O, Ljubenkov I, Roje-Bonacci T (2006) Karst flash floods: an example from the Dinaric karst (Croatia). Nat Hazards Earth Syst Sci 6:195–203. https://doi.org/10.5194/nhess-6-195-2006

Braud I, Ayral PA, Bouvier C, Branger F, Delrieu G, Le Coz J, Nord G, Vandervaere JP, Anquetin S, Adamovic M, Andrieu J, Batiot C, Boudevillain B, Brunet P, Carreau J, Confoland A, Didon-Lescot JF, Domergue JM, Douvinet J, Dramais G, Freydier R, Gérard S, Huza J, Leblois E, Le Bourgeois O, Le Boursicaud R, Marchand P, Martin P, Nottale L, Patris N, Renard B, Seidel JL, Taupin JD, Vannier O, Vincendon B, Wijbrans A (2014) Multi-scale hydrometeorological observation and modelling for flash-flood understanding. Hydrol Earth Syst Sci 11:1871–1945. https://doi.org/10.5194/hessd-11-1871-2014

BRGM (2017a) Dossier du sous-sol BSS002GNMG, source du Lez [Base record for station BSS002GNMG, Lez Spring]. http://ficheinfoterre.brgm.fr/InfoterreFiche/ficheBss.action?id=BSS002GNMG. Accessed January 2017

BRGM (2017b) Dossier du sous-sol BSS002ESPJ, Fontaine de Nîmes [Base record for station BSS002ESPJ, Fontaine de Nîmes spring]. http://ficheinfoterre.brgm.fr/InfoterreFiche/ficheBss.action?id=BSS002ESPJ. Accessed January 2017

BRGM (2017c) Dossier du sous-sol BSS002ESQL, Aven du Pont des neuf arcades [Base record for station BSS002ESQL, Pont des neuf arcades sinkhole]. http://ficheinfoterre.brgm.fr/InfoterreFiche/ficheBss.action?id=BSS002ESQL. Accessed January 2017

Coble PG (1996) Characterization of marine and terrestrial DOM in seawater using excitation-emission matrix spectroscopy. Mar Chem 51:325–346. https://doi.org/10.1016/0304-4203(95)00062-3

Durepaire X, Batiot-Guilhe C, Bailly-Comte V, Brunet P (2014) Suivi en continu de la MON fluorescente à l'aide d'un fluorimètre de terrain: implications pour le suivi des traçages artificiels [Continuous monitoring of fluorescent NOM using a field fluorometer: implications for tracer test monitoring]. 24ème Réunion des Sciences de la Terre (RST), Pau, France, October 2014. https://rst2014-pau.sciencesconf.org/conference/rst2014-pau/rstabstractsnum.pdf. Accessed January 2017

Erostate M, Bailly-Comte V, Batiot-Guilhe C, Durepaire X (2016) Relationships between natural fluorescence and organic matter content based on sampling and in-situ monitoring of groundwater: application to the karst systems of the Lez and Fontaine de Nîmes springs. 43rd IAH Congress, Montpellier, France, 25–29 September 2016

Fleury P, Ladouche B, Conroux Y, Jourde H, Dörfliger N (2009) Modelling the hydrologic functions of a karst aquifer under active water management: the Lez Spring. J Hydrol 365(3–4):235–243. https://doi.org/10.1016/j.jhydrol.2008.11.037

Fleury P, Maréchal JC, Ladouche B (2013) Karst flash-flood forecasting in the city of Nîmes (southern France). Eng Geol 164:26–35

Hudson N, Baker A, Reynolds D (2007) Fluorescence analysis of dissolved organic matter in natural, waste and polluted waters: a review. River Res Appl 23:631–649. https://doi.org/10.1002/rra.1005

Jourde H, Batiot-Guilhe C, Bailly-Comte V, Bicalho C, Blanc M, Borrell V, Bouvier C, Boyer J-F, Brunet P, Cousteau M, Dieulin C, Gayrard E, Guinot V, Hernandez F, Siou KAL, Johannet A, Leonardi V, Mazzilli N, Marchand P, Patris N, Pistre S, Seidel J-L, Taupin JD, Van-Exter S (2011) The MEDYCYSS observatory, a Multi scalE observatory of flooD dYnamiCs and hYdrodynamicS in karSt (Mediterranean border southern France). In: Lambrakis N, Stournaras G, Katsanou K (eds) Advances in the research of aquatic environment. Environmental Earth Sciences. Springer, Heidelberg, Germany

Jourde H, Lafare A, Mazzilli N, Belaud G, Neppel L, Dörfliger N, Cernesson F (2014) Flash flood mitigation as a positive consequence of anthropogenic forcing on the groundwater resource in a karst catchment. Environ Earth Sci 71:573–583. https://doi.org/10.1007/s12665-013-2678-3

Kreft A, Zuber A (1978) On the physical meaning of the dispersion equation and its solutions for different initial and boundary conditions. Chem Eng Sci 33(11):1471–1480

Lacroix M, Rodet J, Wang HQ, Masséi N, Dupont JP (2000) Origin of suspended particulate matter in a karstic aquifer system: contribution of the microgranulometry. C R Acad Sci 330(5):347–354

Lapworth DJ, Goody DC, Butcher AS, Morris BL (2008) Tracing groundwater flow and sources of organic carbon in sandstone aquifers using fluorescence properties of dissolved organic matter (DOM). Appl Geochem 23:3384–3390

Lapworth DJ, Gooddy DC, Allen D, Old GH (2009) Understanding groundwater, surface water and hyporheic zone biogeochemical processes in a chalk catchment using fluorescence properties of dissolved and colloidal organic matter. J Geophys Res 114(10):456–462. https://doi.org/10.1029/2009JG000921

Leonardi V, Jourde H, Dausse A, Dörfliger N, Brunet P, Maréchal J-C (2013) Apport de nouveaux traçages et forages à la connaissance hydrogéologique de l'aquifère karstique du Lez [Using tracer tests

and new wells to improve the knowledge of the Lez karst system hydrogeological functioning]. Karstologia 62:7–14

Lepiller M (2001) Traçages appliqués à la dynamique des aquifères: possibilités et limites [Tracer tests applied to groundwater flow dynamics: possibilities and limits]. Géologues 129:79–84

Maréchal J-C, Petit V, Ladouche B (2004) Synthèse des connaissances géologiques et hydrogéologiques sur le bassin d'alimentation de la Fontaine de Nîmes [Synthesis of geological and hydrogeological knowledge on the recharge area of the Fontaine de Nîmes karst spring]. BRGM/RP-53422-FR, BRGM, Orleans, France, 75 pp

Maréchal J-C, Ladouche B, Dörfliger N (2008) Karst flash flooding in a Mediterranean karst, the example of Fontaine de Nîmes. Eng Geol 99:138–146

Maréchal J-C, Ladouche B, Batiot-Guilhe C, Borrell-Estupina V, Caballero Y, Cernesson F, Dörfliger N, Fleury P, Jay-Allemand M, Jourde H, Leonardi V, Malaterre P-O, Seidel J-L, Vion P-Y (2014) Projet gestion multi-usages de l'hydrosystème karstique du Lez: synthèse des résultats et recommandations [Multi-purpose management project of the Lez karst hydrosystem: summary of results and recommendations]. Rapport BRGM/RP-61051-FR, BRGM, Orleans, France, 126 pp

Meus Ph, Käss W, Schnegg P-A (2006) Background and detection of fluorescent tracers in karst groundwater. In: Duran JJ, Andreo B, Carrasco F (eds) Karst, climate change and groundwater, vol 18. Hidrogeologia y Aguas Subterraneas, IGEM, Madrid, pp 65–75

Mudarra M, Andreo B, Baker A (2011) Characterisation of dissolved organic matter in karst spring waters using intrinsic fluorescence: relationship with infiltration processes. Sci Total Environ 409:3448–3462

Mull DS, Liebermann TD, Smoot JL, Woosley LH (1988) Application of dye-tracing techniques for determining solute-transport characteristics of ground water in karst terranes. US Geological Survey Water Resources Division, Atlanta, GA

Quiers M, Batiot-Guilhe C, Bicalho C, Perette Y, Seidel JL, Van-Exter S (2013) Characterisation of rapid infiltration flows and vulnerability in karst aquifer using a decomposed fluorescence signal of dissolved organic matter. Environ Earth Sci 71:553–561. https://doi.org/10.1007/s12665-013-2731-2

Sadar M (2004) Making sense of turbidity measurements: advantages in establishing traceability between measurements and technology. 2004 National Monitoring Conference: Building and Sustaining Successful Monitoring Programs, NWQC, US Geological Survey, Reston, VA

Schnegg P-A, Dörfliger N (1997) An inexpensive flow-through field fluorimeter. In: Proceedings of the 12th Int. Congress of Speleology, vol 2. La Chaux-de-Fonds, Switzerland, August 1997, pp 47–50

Schnegg P-A, Flynn R (2002) Online field fluorometers for hydrogeological tracer tests. In: Isotope und Tracer in der Wasserforschung, vol 19. Technische Universität Bergakademie Freiberg, Germany, pp 29–36

Schnegg P-A, Le Doucen O (2006) Multispectral field fluorometer for tracer tests in waters of high natural fluorescence. 3rd Int. Symp. on Karst. Málaga Spain, 2006

Schnegg P-A, Thueler L (2012) Application of a multi-LED field fluorometer for simultaneous detection of hard to separate dye tracers and fluocapteurs. XI Congreso Latino-Americano de Hidrogeologia, Cartagena de Indias, Colombia, 19–24 August 2012

Smart PL, Finlayson BL, Rylands WD, Ball CM (1976) The relation of fluorescence to dissolved organic carbon in surface waters. Water Res 10:805–811

Thiery D, Berard P (1984) Alimentation en eau de la ville de Montpellier (34) Captage de la source du Lez Étude des relations entre la source et son réservoir aquifère [Water supply of the city of Montpellier (Herault Dept., France) - Lez karst spring: study of the relationships between the spring and the aquifer reservoir]. Report no. 3, BRGM 84 AGI 175 LRO/EAU, BRGM, Orleans, France

Zepp RG, Sheldon WM, Moran MA (2004) Dissolved organic fluorophores in southeastern US coastal waters: correction method for eliminating Rayleigh and Raman scattering peaks in excitation–emission matrices. Mar Chem 89:15–36. https://doi.org/10.1016/j.marchem.2004.02.006